THE PROTEIN SOCIETY

Non-allosteric enzyme switches possess larger effector-induced changes in thermodynamic stability than their non-switch analogs

Jay H. Choi, Angela San, and Marc Ostermeier*

Department of Chemical & Biomolecular Engineering, Johns Hopkins University, Baltimore, Maryland 21212

Received 6 July 2012; Revised 5 February 2013; Accepted 7 February 2013
DOI: 10.1002/pro.2234
Published online 12 February 2013 proteinscience.org

Abstract: The ability to regulate cellular protein activity offers a broad range of biotechnological and biomedical applications. Such protein regulation can be achieved by modulating the specific protein activity or through processes that regulate the amount of protein in the cell. We have previously demonstrated that the nonhomologous recombination of the genes encoding maltose binding protein (MBP) and TEM1 β-lactamase (BLA) can result in genes that confer maltose-dependent resistance to β-lactam antibiotics even though the encoded proteins are not allosteric enzymes. We showed that these phenotypic switches—named based on their conferral of a switching phenotype to cells—resulted from a specific interaction with maltose in the cell that increased the switches cellular accumulation. Since phenotypic switches represent an important class of engineered proteins for basic science and biotechnological applications *in vivo*, we sought to elucidate the phenomena behind the increased accumulation and switching properties. Here, we demonstrate the key role for the linker region between the two proteins. Experimental evidence supports the hypothesis that in the absence of their effector, some phenotypic switches possess an increased rate of unfolding, decreased conformational stability, and increased protease susceptibility. These factors alone or in combination serve to decrease cellular accumulation. The effector functions to increase cellular accumulation by alleviating one or more of these defects. This perspective on the mechanism for phenotypic switching will aid the development of design rules for switch construction for applications and inform the study of the regulatory mechanisms of natural cellular proteins.

Keywords: allostery; β-lactamase; domain fusion; maltose binding protein; phenotypic switch; protein switch

Introduction

The regulation of protein activity in the cell by biological molecules or cellular processes is central to life. The ability to create regulatable proteins, also known as protein switches, has many biotechnological, biomedical, and basic science applications.[1] One approach for creating such protein switches is to fuse two independent proteins, one that has the function to be regulated (the output domain) and the other that possesses the ability to recognize the desired regulating signal (the input domain). We have previously demonstrated that this approach

Abbreviations: BLA, β-lactamase; CD, circular dichroism; GFP, green fluorescent protein; IPTG, isopropyl-β-D-thiogalactopyranoside; MBP, maltose binding protein; MIC, minimum inhibitory concentration; PCR, polymerase chain reaction.

Additional Supporting Information may be found in the online version of this article.

Grant sponsor: Defense Threat Reduction Agency; Grant number: HDTRA1-09-1-0016.

*Correspondence to: Marc Ostermeier, Johns Hopkins University, Maryland Hall, Room 221, 3400 N. Charles Street, Baltimore, MD 21218. E-mail: oster@jhu.edu

can create protein switches that function as heterotropic allosteric enzymes in which binding of a small molecule to the input domain modulates the activity of the output domain via conformational changes that propagate from the input domain to the output domain.[2–4]

Our directed evolution approach for engineering protein switches involves two important steps: (1) creation of a library of gene fusions through random insertion of one gene into the other and circular permutation of the insert gene to vary the fusion geometry, and (2) genetic selections or screens to identify protein switches among the majority of nonfunctional constructs. The genetic selection of protein switches requires a selectable phenotype to identify the switching activity modulated by the input signal. We have previously designed a genetic circuit that enables the selection of cells that lack beta-lactamase activity.[5] When combined in series with a positive selection for conferral of resistance to beta-lactam antibiotics, this negative selection facilitates identification of protein switches with regulatable β-lactamase activity.[5] However, a selection based on cellular phenotype can result in the identification of gene fusions that confer a switching behavior to cells by means other than effector-induced modulation of a protein's specific activity. For example, the desired phenotype could arise by mechanisms involving the regulation of transcription, translation, protein targeting, protein degradation, and intra-/intercellular interactions with other molecules such as inhibitors and activators. We applied our two-tier selection to identify maltose-activated beta-lactamases from a library of gene fusions between TEM-1 beta-lactmase (BLA) and maltose binding proteins (MBP). The majority of the gene fusions selected from the two-tier genetic selection did not to encode allosteric enzymes; however, they still conferred to *E. coli* an increase in ampicillin (Amp) resistance in the presence of maltose.[5,6] This phenomena arose by an increase in cellular accumulation of the fusion proteins in the presence of maltose–an accumulation arising from a specific interaction between the switch and maltose.[6] We termed these switches "phenotypic switches." The similar ligand-dependent behavior of engineered fusion proteins have been previously reported in different systems, and these unique characteristics of fusion proteins have been used to develop screening methods for ligand binding and protein stability.[7–9] Ligand-induced upregulation of constitutively active mutant form of β_2-adrenoceptor tagged with the luciferase at the C-terminal, resulted in elevated levels of luciferase activity, and this system was used to develop high-throughput assay to monitor ligand binding to G-protein-coupled receptor.[7] In other systems, the fluorescent sensitivity of green fluorescent protein (GFP) to the ligand-induced folding of proteins fused to its N-terminus was used to develop high-throughput method to monitor ligand binding and thermal stability of proteins of interest such as steroid receptor and glycerol kinase.[8,9] The prevalence of the gene fusions that confer switching behavior in the library of nonhomologously recombined genes has important implications for construction and application of protein switching. If the engineered protein switch is designed to act in an intracellular environment as a cellular reporter of the effector or as a selective therapeutic protein, then these phenotypic switches can be as effective and useful as allosteric switches. Thus, these phenotypic switches represent an important class of switch proteins for *in vivo* applications. We have recently constructed switches that activate prodrugs in a cancer marker-dependent fashion that behave as phenotypic switches whose cellular accumulation is cancer-marker dependent.[10]

In this study, we address the mechanism of phenotypic switches. We constructed a set of MBP-BLA fusion proteins intermediate between two previously described fusions: phenotypic switch Ph7 and a similar fusion, c4, that largely lacked any switch behavior. We examined the cellular accumulation level, proteolytic susceptibility, thermodynamic stability, folding kinetics, and enzymatic activity of these phenotypic switches in the presence and absence of maltose. We found that the phenotype conferred by these gene fusions is related to changes in the conformational stability of the fusion proteins in a ligand-dependent manner. Evidence suggests that a switching behavior can be dictated by a protein's thermodynamic stability and unfolding rate in the absence of effector, which results in effector-dependent changes in proteolytic susceptibility and cellular protein accumulation.

Results

Linker length inversely correlates with switching activity for variants of Ph7 and c4

Phenotypic selection is a powerful method for the identification of proteins with altered structure, stability, and function.[11–13] In previous studies, we have identified fusion proteins with regulatable β-lactamase activity from the genetic selection based on phenotypes. Ph7 and c4 are previously described fusion proteins in which BLA is inserted after residue 316 of MBP (Table I).[6] The differences in the primary sequence between Ph7 and c4 occur after the BLA domain: Ph7 continues on with residues 318–370 of MBP, whereas c4 contains the linker sequence DKT before residues 319–370 of MBP. The ampicillin resistance conferred by c4 is largely independent of maltose, whereas Ph7 confers a maltose-dependent resistance to ampicillin. The

Table I. *Primary Sequence of Fusion Proteins Used in this Study*

Protein	Protein sequence[a]
c4	MBP[1–316]-BLA[24–286]-DKT-MBP [319–370]-6xHis
Ph7+DK	MBP[1–316]-BLA[24–286]-DK-MBP [318–370]-6xHis
Ph7+D	MBP[1–316]-BLA[24–286]-D-MBP [318–370]-6xHis
Ph7	MBP[1–316]-BLA[24–286]-MBP[318–370]-6xHis
Ph7Δ318	MBP[1–316]-BLA[24–286]-MBP[319–370]-6xHis

[a] Based on gene sequencing.

ampicillin resistance of Ph7-expressing cells is compromised in the absence of maltose but restored to approximately c4 levels by the addition of maltose.[6] This phenomenon, which we termed phenotypic switching, primarily manifests through the increased cellular accumulation of Ph7 in the presence of maltose and not through Ph7 acting as an allosteric enzyme with maltose as a positive effector. This striking contrast in properties with only differences in the linker residues provided an excellent opportunity to investigate the role of the linker residues in phenotypic switch behavior and the mechanisms leading to Ph7's phenotypic switch properties.

We constructed a series of variants intermediate between c4 and Ph7 (Table I). Since Ph7 possessed but c4 lacked residue A318 of the MBP domain, we first mutated the threonine in the linker of c4 to alanine. This variant (Ph7+DK) can be thought of as Ph7 in which a DK linker has been inserted between the BLA and MBP[318–370]. We next removed the lysine to shorten the linker (Ph7+D). Finally, we removed the DKT linker from c4, and the resulting construct (Ph7Δ318) can also be viewed as removing MBP residue A318 from Ph7.

BL21 cells were transformed with plasmids bearing these gene variants. The genes' abilities to confer maltose-dependent minimum inhibitory concentration (MIC_{Amp}) were tested in a 5 mL liquid culture [Fig. 1(A)]. The maltose-dependent increase in MIC_{Amp} of both c4 (two fold) and Ph7 (64-fold) was higher in BL21 than in RH22 cells [6] (1- to 2-fold and 16- to 32-fold respectively), indicating that the phenotypic switching ratio is strain dependent and suggesting that cellular factors play a role in the phenomenon. The progressive addition of linker residues to Ph7 decreased phenotypic switching. This decrease resulted more from alleviating the defect in MIC_{Amp} in the absence of maltose, although the MIC_{Amp} increased with linker length both in the absence and presence of maltose (Supporting Information Table 1). Similarly, the pattern of ampicillin resistance of Ph7Δ318 illustrated that removing the DKT linker from c4 increased the switching ratio to that of Ph7, though overall levels of MIC_{Amp} were reduced compared to Ph7.

Maltose's effect on cellular accumulation correlates with switching phenotype

We used western blots to quantify the effect of maltose on the cellular accumulation of the variants. We have previously shown maltose's effect on phenotypic switches derives from effects on the protein level and not from effects on transcription.[6] Cellular

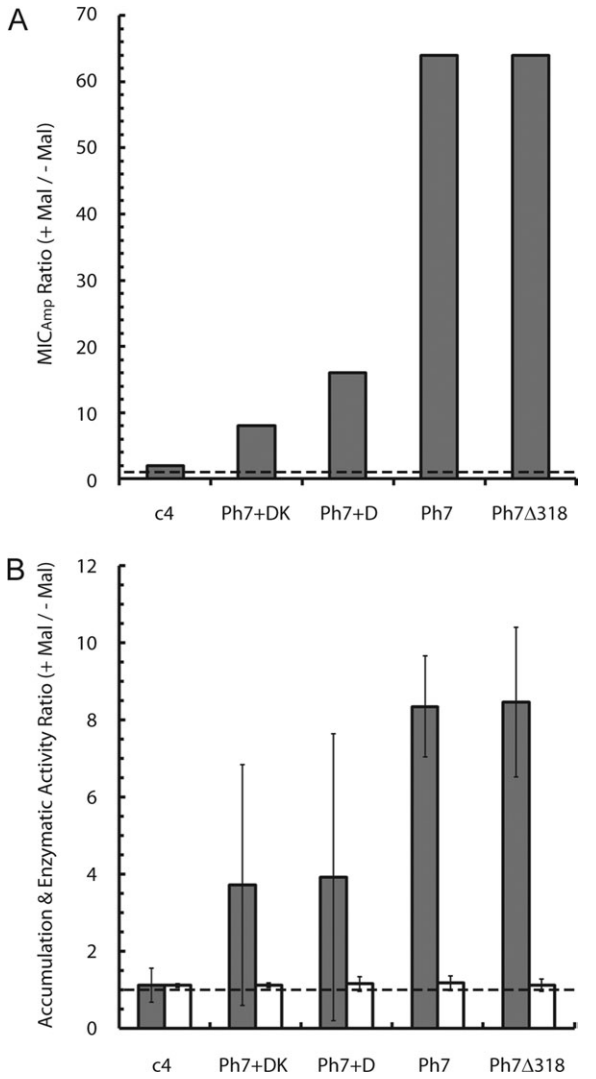

Figure 1. The effect of maltose on the engineered genes and proteins. A: Fold increase in ampicillin resistance for cells grown in the presence of maltose compared to cells grown in the absence of maltose. The ratio (+maltose/-maltose) was calculated using median MIC_{Amp} from three independent trials in the absence and presence of 5 mM maltose (Supporting Information Table 1). B: The maltose-induced fold increase in cellular accumulation (black bars) and *in vitro* enzymatic activity (white bars). The accumulation ratio (+maltose/-maltose) was calculated by quantification of western blots of SDS-PAGE gels of the soluble fraction of cell lysates from cells grown in the absence or presence of 5 mM maltose. The enzymatic activity ratio (+maltose/-maltose) was calculated from the initial rates of 200 μM ampicillin hydrolysis measured in the absence and presence of 5 mM maltose. Error bars represent the standard deviation calculated from three independent trials.

accumulation levels in the absence and presence of maltose were determined under the same conditions as the MIC assays, as previously described.[6] The western blots showed that the addition of maltose increased the cellular accumulation of Ph7 about eight fold but did not increase the cellular accumulation of c4 [Fig. 1(B)]. Although the difference in accumulation was highly variable for some fusion proteins, maltose's effects of the cellular accumulation of the variants qualitatively mirrored the MIC_{Amp} ratios. This correlation between protein accumulation ratio and MIC_{Amp} ratio suggests that increased cellular accumulation of proteins in the presence of maltose significantly contributes to the maltose-dependent MIC_{Amp} phenotype. This observation is consistent with our previous study of other phenotypic switches.[6]

None of the switch proteins behave as allosteric enzymes in vitro

To investigate whether the variants exhibit a maltose-induced allosteric property, the initial rates of the ampicillin hydrolysis in the presence and absence of maltose were determined [Fig. 1(B) and Supporting Information Table 2]. The ampicillin concentration tested (70 μg/mL) is within the range used in the MIC assays for ampicillin (0 to 2048 μg/mL). The initial rates remained approximately the same for all of the variants, and maltose did not significantly alter the ampicillin hydrolysis activity. Thus, maltose is not a heterotropic allosteric effector of these proteins, and the switching phenotype must arise solely from maltose-dependent differences in cellular accumulation.

Phenotypic switch behavior correlates with increased proteolytic susceptibility

An increase in the switching phenotype correlates with an increase in maltose's effect on cellular accumulation. This increase in the accumulation ratio primarily results from a large decrease in accumulation in the absence of maltose. A possible explanation for the decrease in accumulation is an increased susceptibility to cellular proteases. Since it is difficult to examine a proteins' susceptibility to all constituent proteases in the bacterial cell, we conducted an *in vitro* proteolysis experiment on the purified fusion proteins using thermolysin as the proteolytic enzyme. Since thermolysin has a broad specificity (it hydrolyzes peptide bonds at hydrophobic residues), it can provide a general indication of how susceptible proteins are to proteolytic degradation. Purified variants were incubated with thermolysin (with and without maltose) at 37°C, followed by quenching with EDTA. We examined the digested proteins by sodium dodecyl sulfate polyacrylamide gel electrophoresis (SDS-PAGE), and quantified the band intensities to determine the relative protease susceptibility against thermolysin (Fig. 2). Undigested proteins showed no proteolytic degradation in the absence of thermolysin. However, with thermolysin proteolysis, Ph7 showed greater degradation of the full-length protein than c4, as judged by the band intensities at ~70 kDa. The addition of linker residues progressively decreased Ph7's susceptibility to thermolysin degradation. Degradation of all proteins was less in the presence of maltose, suggesting that specific interactions with maltose may partially protect the proteins from thermolysin digestion. However, no correlation between the degree of protection

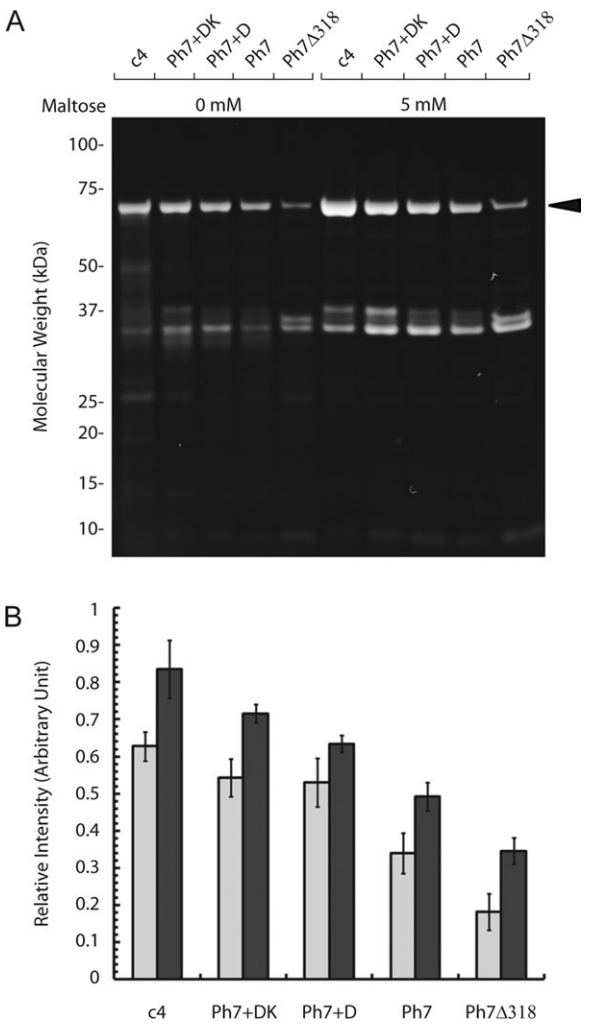

Figure 2. Proteolytic susceptibility measured by pulse proteolysis. A: SDS-PAGE gel of proteolyzed samples of the indicated proteins subjected to thermolysin digestion. Purified proteins were treated with thermolysin in 50 mM sodium phosphate buffer for 1 min at 37°C in the presence or absence of 5 mM maltose. The arrow indicates unproteolyzed proteins. B: Quantification of the relative band intensities of the unproteolyzed proteins in protease digestion experiments from images of SDS-PAGE gels. Error bars represent the standard deviation calculated from three independent trials. SDS-PAGE analysis of the proteins before addition of protease is shown in Supplementary Figure 2.

afforded by maltose and the switching phenotype was apparent.

In addition to the band at ~70 kDa, bands were visible in the 35–40 kDa range. The bands were more prominent for proteins incubated with maltose prior to proteolysis. The size of bands decreased with linker length from c4 to Ph7 / Ph7Δ318; however, the decrease was much greater than could be explained by the shorter linker alone. A band at ~30 kDa was also visible in most lanes but with markedly higher intensity in the presence of maltose. Although thermolysin has a molecular weight of ~33 kDa, controls of thermolysin in the absence of fusion proteins indicated thermolysin should not be clearly visible due the low amount of thermolysin used in this study (data not shown). The expected molecular weight of the MBP domain of the variants is ~35 or ~40 kDa, depending on whether or not the C-terminal domain (MBP318–370) is included, suggesting that these bands could correspond to fragments of MBP domain, protected from further protease degradation. In addition, the expected molecular weight of the BLA domain is ~30 kDa, suggesting that the lower bands could correspond to fragments of the BLA domain.

Western blots using anti-His, anti-MBP, and anti-BLA antibodies showed that the higher molecular weight fragments in the 35–40 kDa range contain fragments of both the MBP and BLA domains. Provided that the band is a single species, this would correspond to the C-terminal fragment of the proteins. Based on size, this fragment would contain the entire BLA domain and correspond to a cleavage at about the first fusion site between the MBP and BLA domains. Interestingly, the lower molecular weight fragment at ~30 kDa only reacted with anti-BLA antibodies and only in samples proteolyzed in the absence of maltose (Supporting Information Fig. 3). Thus, the presence of maltose alters the identity of the major proteolytic fragments, either by changing the primary digestion site(s) or by altering the rate of proteolysis at certain location(s). The later possibility is consistent with the increased proteolytic resistance of all variants in the presence of maltose.

Increased linker length increases the thermodynamic stability in the absence of maltose

Fusion of an enzyme with a thermostable protein can serve to stabilize the enzyme domain,[14] indicating a link between the stability of the enzyme domain and the stability of the protein to which it is fused. The effects of a domain fusion and connecting linkers in engineered fusion protein on stability and folding have been studied in different systems.[15,16] Watanabe *et al.* showed that thermostability of engineered 12-membered ring structure of the bacterial protein TRAP can be significantly improved by relieving mechanical strain into the system with increasing length of the peptide linker between subunits.[15] In the study of folding and unfolding equilibrium and kinetics of the engineered ubiquitin–ubiquitin interacting motif fusion protein, it was found that the stabilization of the fusion protein was due to the decrease in the unfolding rate.[16] In addition, association with ligand often increases the apparent stability of the protein by selectively binding to the folded state of the protein in its native conformation.[17–19] Changes in the thermodynamic stability of proteins due to ligand binding coupled with protein folding equilibrium have been studied previously.[20–24]

The thermodynamic stability of the variants at 37°C was probed by urea-induced unfolding and monitored by tryptophan fluorescence spectroscopy in order to investigate the relationship between thermodynamic stability and phenotypic switch behavior. A decrease in fluorescence intensity as a result of urea-induced unfolding correlated with changes in ellipticity by circular dichroism (CD) spectroscopy, indicating that the change in fluorescence spectra reflects changes in structure (Fig. 3). Upon excitation at 280 nm, maximal fluorescent emission was observed in a 340–345 nm range. Upon addition of urea and subsequent protein unfolding, a shift of the emission spectrum within the 340–345 nm range and a decrease of fluorescence intensity were observed.

To determine whether the unfolding of the fusion proteins was reversible, urea-induced unfolding and refolding of c4 and Ph7 were monitored (Fig. 4). In the absence of maltose, denaturation and renaturation curves were superimposable, suggesting that the folding of both c4 and Ph7 was reversible in the equilibrium state. Guanidine hydrochloride was also used as a chemical denaturant to confirm the reversibility of the protein folding (data not shown). The presence of maltose shifted the denaturation midpoint to significantly higher urea concentrations (~3.5M urea); however, unlike in the absence of maltose, the renaturation was not superimposable, with a refolding midpoint < 2M urea.

Urea-induced unfolding transitions were measured in order to estimate relative thermodynamic stability of the variants in the absence and presence of maltose. In the absence of maltose, the unfolding transition curves showed a potential three-state behavior for all proteins. A slightly curved plateau region was observed between 1.25 and 2.5M urea in all variants, followed by the second transition, indicating a intermediate state of conformation. The first transitions were observed at $[\text{Urea}]_{1/2}$ concentrations between 0.8 and 1.25M, while the second transitions were observed at $[\text{Urea}]_{1/2}$ concentrations between 1.8 and 2.8M. For the first transition, Ph7 had the lowest $[\text{Urea}]_{1/2}$ and the progressive addition

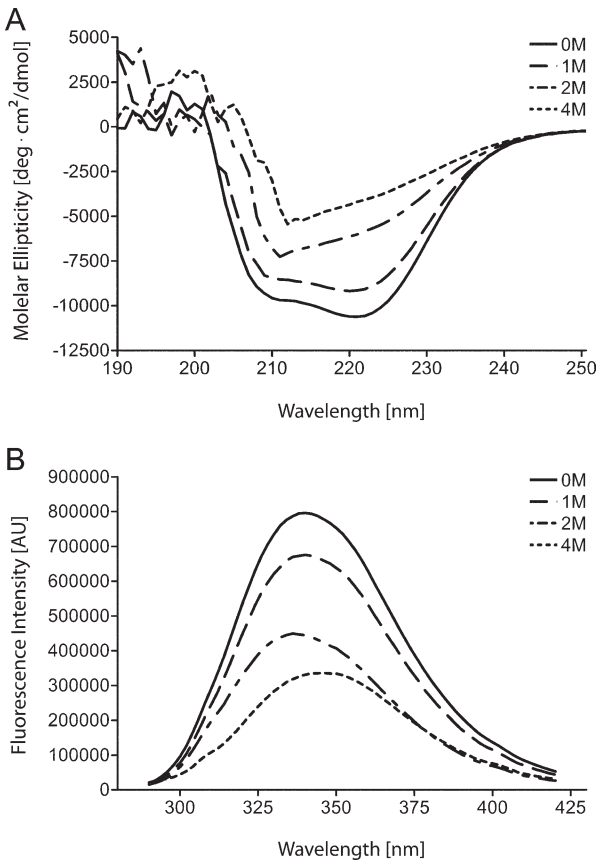

Figure 3. Spectroscopic characterization of c4. CD spectra (A) and fluorescence emission spectra (B) of c4 in its native state (solid line) and in its urea-denatured states (dotted lines) were recorded in 50 mM sodium phosphate, pH 7.5 containing no denaturant or 1 to 4M urea. CD spectra are the average of three scans taken at a spectral bandwidth of 1 nm with 2-sec integration time. Fluorescence emission spectra were recorded with excitation at 280 nm and spectral bandwidths of 2 nm (excitation) and 4 nm (emission). All spectra were recorded at 37°C and buffered-corrected.

of linker residues gradually raised the transition midpoint. c4 had the highest midpoint, which was about 0.5M urea higher than Ph7's midpoint. The second transitions were less defined and comparisons between the variants could not be made. Despite the differences in transition midpoints of c4, Ph7+DK, Ph7+D, and pH7, all showed similar overall transition curves, whereas Ph7Δ318 showed less distinct separation between the first and second denaturation transition. The presence of maltose changed the urea denaturation behavior to the common two-state transition behavior and shifted the apparent denaturation midpoints of all variants to ~3.5M urea.

The results indicate that the addition of linker residues to Ph7 increases its thermodynamic stability in the absence of maltose, with longer linkers causing the most stabilization. The relative thermodynamic stability predicts the relative accumulation levels and thermolysin susceptibility in the absence of maltose. The addition of maltose stabilizes all variants up to the same level, but since Ph7 is the most destabilized in the absence of maltose, maltose has the greatest effect on the stability of Ph7. Ligand-induced increases in the thermodynamic stability could contribute to the increased protein accumulation and decreased protease susceptibility.

Phenotypic switches unfold faster in the absence of maltose

Protein–ligand association generally affects both the stability and unfolding of proteins. Ligand binding often decreases unfolding rates of proteins in many cases including MBP; however, it rarely increases folding rates of proteins.[25–29] We determined the

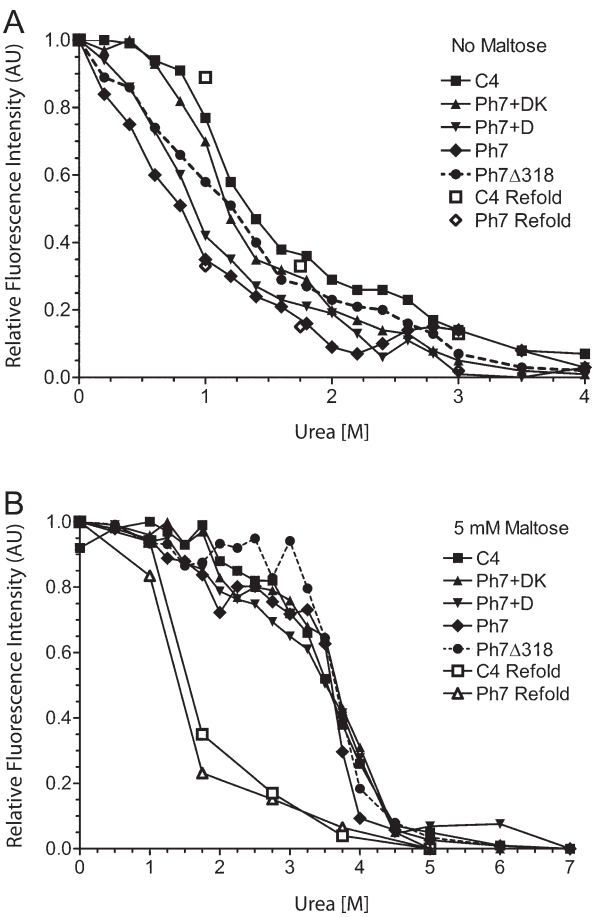

Figure 4. Unfolding/refolding equilibrium transitions of the engineered proteins. Urea-induced transitions were assessed by the fluorescence emission wavelength at 342 nm and excitation wavelength at 280 nm in the (A) absence and (B) presence of maltose. Solid symbols are for the denaturation and open symbols are for the renaturation. For denaturation, native proteins were mixed and incubated in the 50 mM sodium phosphate buffer, pH 7.5 at 37°C with the urea concentration indicated. For renaturation, proteins previously unfolded in 5M urea were diluted to the final urea concentration indicated. Data represent the combined results from three independent trials.

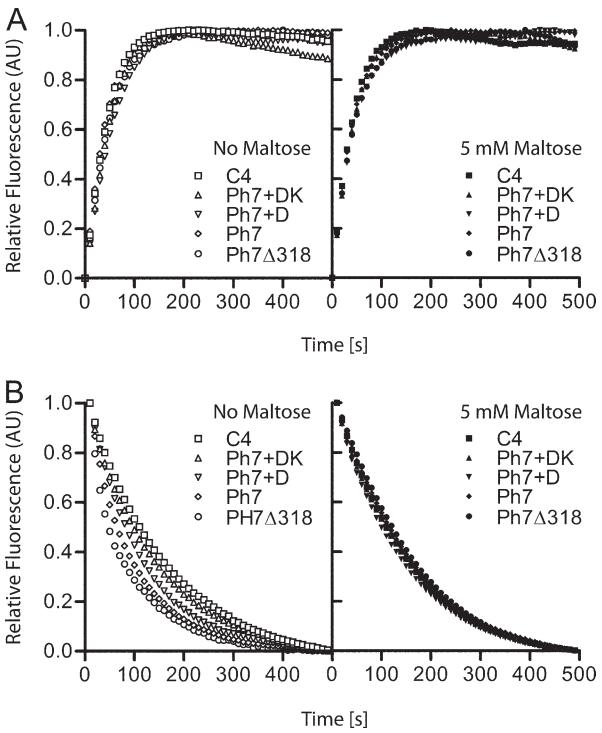

Figure 5. Unfolding and refolding kinetics of the engineered proteins. Kinetics were monitored by tryptophan fluorescence emission at 342 nm and excitation at 280 nm for (A) refolding and (B) unfolding. Solid symbols are for the absence of maltose, and open symbols are for the presence of maltose. Unfolding was initiated by mixing native proteins in 5M urea at 37°C. For refolding, proteins previously unfolded in 5M urea were diluted into 50 mM sodium phosphate buffer, pH 7.5 at 37°C. Fluorescence intensity of the native proteins and unfolded proteins in 5M were normalized to 1.0 and 0, respectively. The data shown is representative of the results of three independent trials. The kinetic parameters determined from the three trials are provided in Supporting Information Table 3.

apparent unfolding and refolding rates of the variants in the absence and presence of maltose at 37°C by intrinsic fluorescence spectroscopy (Fig. 5). For refolding kinetics, we first denatured the proteins in 5M urea–concentrations at which the CD and intrinsic protein fluorescence measurements indicated complete unfolding of the proteins. We initiated refolding by rapid dilution into a neutral buffer. After a burst in fluorescence in the dead-time of manual mixing, the fluorescence signals at the maximum emission wavelength of the native protein increased with a half-time of ~30 sec for all proteins in both the absence and presence of maltose [Fig. 5(A)]. The apparent folding kinetic constant (k_f) was approximated by fitting the plot of fluorescence versus time to a first-order rate equation ($r^2 > 0.98$). All proteins refolded with apparent rate constants of $k_f = \sim 2.0 \times 10^{-2}$ s^{-1} (Supporting Information Table 3). No significant differences were observed in the refolding of proteins in the absence and presence of maltose, suggesting that maltose has no significant effect on the folding rates of any of the proteins.

We initiated unfolding by mixing native proteins in either 3M (for experiments in the absence of maltose) and 5M urea (presence of maltose) and monitored by fluorescence spectroscopy. A rapid decrease in fluorescence was observed with the fluorescence signals at the maximum emission wavelength of the native protein at 342 nm [Fig. 5(B)]. The unfolding kinetic constant (k_u) was approximated by fitting the plot of fluorescence versus time to a first-order rate equation ($r^2 > 0.98$). The unfolding rates in the presence of maltose were the same for all variants. In contrast, in the absence of maltose the progressive removal of linker residues from c4 gradually increased the unfolding rate. The unfolding rate of Ph7 ($k_u = 1.1 \times 10^{-2}$ s^{-1}) was about twice as fast as that of c4 ($k_u = 0.6 \times 10^{-2}$ s^{-1}). This increase in rate constants with deletion of linker residues indicates that the decrease in thermodynamic stability with deletion of linker residues is most likely a result of the increase in the unfolding rate. The increase in unfolding rates may also explain the increased susceptibility to proteolytic degradation. In the presence of maltose, however, the variants showed no apparent differences in folding rates, consistent with the same denaturation transition for all variants in the presence of maltose. For Ph7, Ph7Δ318 and Ph7+D, unfolding rates decreased in the presence of maltose, suggesting that ligand binding slowed unfolding of variants. However, maltose did not significantly change the unfolding rate of c4 and Ph7+DK (i.e. longer linker variants), inconsistent with the increased stability of these variants in the presence of maltose shown in the urea denaturation experiments. This apparent inconsistency may result from experimental limitations in monitoring the change in stability and unfolding rate of each domain of the fusion proteins.

Discussion

Changes in the linker corresponding to intermediates between c4 and Ph7 dramatically changed the phenotypic switching magnitude from two fold to 64-fold, illustrating the importance of the linker residues in ligand-dependent switching activity of fusion proteins in the cellular environment. Starting from the weak switch c4 (two fold), the threonine to alanine substitution in the DKT linker to create Ph7+DK lowered the MIC_{Amp} four fold in the absence of maltose, while MIC_{Amp} in the presence of maltose remained unchanged, resulting in an eight-fold switch. This result indicates that changes in the sequence of the connecting regions can modulate switching activity. Subsequent deletions in the linker to create Ph7+D and then Ph7, resulted in a dramatic decrease of MIC_{Amp} in the absence of maltose but a moderate decrease in the presence of

maltose. Overall this contributed to a further eight-fold increase in switching activity and a combined 64-fold effect of maltose on the MIC_{Amp} of cells. This finding indicates that the length of the linker also has a significant contribution to switching activity.

The primary mechanism by which deletion of the linker residues resulted in a large increase in the phenotypic switch ratio was the large decrease in the switches accumulation in the absence of maltose. One of the possible mechanisms for decreasing cellular accumulation of proteins is the increased degradation of proteins by cellular proteases. Upon fusion of two different proteins, the distortion of the wild-type folds can result in exposure of regions that can be protease-sensitive. These unstructured regions can also have entropic contributions to the protein fold that lower overall stability and increase proteolytic susceptibility. Maltose-binding to these fusion proteins can modulate the stability or the availability of the proteolytically sensitive sites through maltose-induced conformational changes in the protein. The effect of variations in the linker on thermolysin susceptibility suggests that the linker in the fusion proteins may either be a specific target to certain proteases in the cell or be involved in changing the overall stability of proteins. Thermolysin proteolysis resulted in different sized fragments of fusion proteins in the ~35–40 kDa range among the variants. The difference in size of these bands among the variants suggests that differences in the linkers may cause exposure of different regions and thus cleavage at different residues. Since thermolysin has a broad specificity, this effect does not manifest in maltose having a significant effect on the degradation rates of the switch variants. However, a cellular protease with a higher degree of specificity may preferentially cleave some variants in a maltose-dependent manner depending on whether its cleavage site is exposed. The decrease in protease susceptibility in the presence of maltose indicates that maltose-induced conformational change increases proteolytic stability in general, presumably by decreasing the availability of protease-sensitive sites.

The fusion of unrelated proteins likely results in destabilization such that a fusion protein may have a lower thermodynamic stability compared to its parental proteins. On the other hand, a ligand-binding event often stabilizes proteins by its specific interaction with proteins.[30] Thus, this combination of phenomenon could account for the decreased accumulation and increased protease susceptibility of c4 linker variants in the absence of maltose and the increased accumulation and the decreased protease susceptibility in the presence of maltose. Increased stability can result in an increase in accumulation and antibiotic MIC of fusion proteins involving BLA.[31] Also, the temperature-induced unfolding of c4 and phenotypic switches Ph8 and MBP317–347 showed that the fusion of MBP and BLA resulted in a significantly lower melting temperature (T_m) when compared to those of their parental proteins.[6] All three proteins had approximately the same T_m in the absence of maltose, and maltose increased the melting temperature of all by about 10°C indicating that the effect of maltose on the melting temperature could not be used to identify phenotypic switches from nonswitches.

Here, we find that in the absence of maltose the urea-induced unfolding of the fusion proteins of MBP and BLA did not fit the simple two-state model of protein folding, but rather appeared to have two regions, perhaps corresponding to the unfolding of each domain. However, maltose binding collapsed the two regions into one resulting in a standard two-state transition behavior, suggesting that the thermodynamic stability of BLA domain is linked to the state of the MBP domain. In addition, denaturation transitions at lower urea concentration in the absence of maltose indicated that better phenotypic switches had a decrease in thermodynamic stability in the absence of maltose but not in the presence of maltose, suggesting that ligand-induced stabilization may recover the stability lost by shortening the linkers. Furthermore, the only significant difference in folding rates of the proteins was that the better phenotypic switches unfolded faster in the absence of maltose. This suggests that the stability differences observed were the results of changes in the rate at which the proteins unfolded in the absence of maltose. This decrease in thermodynamic stability in the absence of maltose may account for the decreased cellular accumulation in the absence of maltose. The decreased accumulation could result from having more unfolded protein that degrades quicker due to exposure of proteolytic sites.

For the phenotypic switch here, it appears the higher rate of unfolding crosses a threshold at which cellular accumulation of the switch is compromised. This increase in the unfolding rate is rescued back across the threshold by the addition of maltose, such that Ph7 accumulates to a higher level. How the increase in the unfolding rate results in lower accumulation is not known, however an increase in proteolytic degradation or other mechanism that changes the state of the protein such that it does not refold (i.e. aggregation, proteosomal degradation, or any protein turnover mechanism) are prime candidates. These mechanisms need not be mutually exclusive and may vary from switch to switch Further understanding the mechanisms of how phenotypic switches work will inform the development design rules for protein switches that could find use as therapeutics or cell-based biosensors.

Materials and Methods

Strains and plasmids

BL21 competent cells purchased from Agilent Technologies. pDIMC8-RHPhc4, a plasmid that contains the c4 gene was previously described.[6]

Site-directed mutagenesis

c4 gene was amplified from pDIMC8-RHPhc4 using a polymerase chain reaction (PCR) with primers that contained 6xHis-tag coding sequence. The amplified PCR product was ligated back into pDIMC8 plasmid, and the resulting plasmid was named pDIMC8-c4h. pDIMC8-c4h was used as a template plasmid DNA to make variants using the QuikChange site-directed mutagenesis method (Agilent Technologies). DNA sequencing of a 2019 bp region containing the targeted codon confirmed mutant clones (Genewiz).

Liquid culture MIC_{Amp} assay

MIC_{Amp} assay was performed as previously described.[6] BL21 cells were transformed with pDIMC8 plasmids containing genes that encode the protein variants. For each overnight culture, 5 mL of tryptone broth (10 g/L tryptone and 10 g/L NaCl) was inoculated by picking a single colony, and incubated in a 37°C shaker for 16–18 h. The optical density at 600 nm (OD_{600nm}) was measured. For MIC_{Amp} assay, approximately 1×10^6 colony forming unit (based on OD_{600nm}) from the overnight culture was added to 5 mL of tryptone medium containing chloramphenicol (Cm, 50 μg/mL), isopropyl-β-D-thiogalactopyranoside (IPTG, 300 μM), Amp (0–8192 μg/mL), and either the absence or presence of 5 mM maltose in each culture tube. Five milliliter cultures were incubated in a 37°C shaker incubator for 18 h, and the OD_{600nm} of each culture was measured. The MIC_{Amp} was defined as the lowest concentration of ampicillin at which the OD_{600nm} was <5 % of the OD_{600nm} in the absence of ampicillin.

Ampicillin hydrolysis enzymatic assay

Enzymatic assays were performed as previously described.[6] Proteins added in 100 mM sodium phosphate buffer, pH 7.5 to the final concentration of 2 nM, and incubated in the absence and presence of 5 mM maltose for 5 min at 37°C. Ampicillin was added to the final concentration of 200 μM. The absorbance at the wavelength of 235 nm was recorded by using a Varian Cary 50 UV-Visible Spectrophotometer (Agilent Technologies) in order to measure the initial rate of ampicillin hydrolysis reaction.

Western blot for quantification of protein accumulation

The previously described method was used for western blotting and quantification of protein accumulation.[6] A total of 6.8×10^8 cells (based on OD_{600nm}) from MIC_{Amp} culture were collected, concentrated by centrifugation, and resuspended in 250 μL of Bugbuster (Agilent Technologies) supplemented with rlysozyme (Agilent Technologies), benzonase nuclease (Agilent Technologies) and protease inhibitors (Sigma). Cells were lysed for 1 h at 4°C, centrifuged, then the soluble fraction was transferred into a new 1.5 mL tube. The soluble lysates were loaded onto a 4%–12% Bis-Tris Gel (Invitrogen) and electrophoresed. Proteins were transferred to PVDF membrane (Bio-Rad) using a semidry transfer cell (Bio-Rad). The membrane was processed following the guidelines of the SNAP-ID system (Millipore). The membrane was blocked with 0.2% milk in Tris buffered saline, 0.05% Tween 20 (TBST) and incubated with anti-His antibody (Invitrogen), followed by washing with TBST. The blot was incubated with 1 mL of WesternC substrate and enhancer (Bio-Rad) and imaged using a ChemiDoc XRS imaging system (Bio-Rad). Quantification of the intensity of bands corresponding to the amount of the proteins was performed using the Quantity One software package (Bio-Rad).

Expression and purification of c4 and c4 variants

Proteins were purified from BL21 cells grown in M9 minimal media[32] containing ammonium chloride (18.5 mM), thiamine (30 μM), $MgSO_4$ (2 mM), $CaCl_2$ (100 μM), fructose (50 mM), 2% glycerol (w/v), and Cm (50 μg/mL). For production of each protein, 1 L of minimal media was inoculated with 10 mL overnight culture of BL21 cells harboring the pDIMC8 plasmid encoding the proteins and shaken at 37°C until the OD_{600} reached 0.7. The culture was induced with 1 mM IPTG and incubated at 25°C for another 48–50 h. After expression, the cells were harvested and resuspended in 10 mL buffer (50 mM sodium phosphate, 150 mM NaCl) and lysed using a French press. Cell lysates were centrifuged at 20,000 g for 1 h. The soluble proteins were purified using the HisTrap (GE Healthcare Life Sciences) and size-exclusion column in the AKTA FPLC purifier system (GE Healthcare Life Sciences). Proteins were concentrated in a storage buffer (50 mM sodium phosphate, 150 mM NaCl, and 20% glycerol) using Amicon centrifugal filter (Millipore). Approximately 5 mg of purified proteins were obtained with >95% purity, estimated by coomassie blue staining of SDS-PAGE gels. Protein concentration was determined using a Nanodrop spectrophotometer (Thermo Scientific) by measuring UV absorbance at 280 nm.

Proteolysis of c4 and c4 linker variants

Proteolysis was carried out using the protocol adopted from the pulse proteolysis method developed by Park *et al.*[19,29,33,34] Proteins were initially

incubated in buffers with no maltose and 5 mM maltose for 30 min at 37°C prior to proteolysis. For proteolysis, thermolysin (10 mg/mL) was added to a final concentration of 0.05 mg/mL, and the solution was incubated for 1 min at 37°C. The reaction solutions were then mixed with 50 mM EDTA (pH 8.0) to quench the proteolysis reaction. Laemmli sample buffer (Bio-Rad) was added to the quenched reaction, and the sample was loaded onto 4%–12% Bis-Tris Gel (Invitrogen) and electrophoresed for 45 min at 190 V. Gels were stained with SYPRO Red fluorescent dye (Invitrogen) and scanned using a ChemiDoc XRS imaging system (Bio-Rad). Band intensities of the intact proteins were quantified with the image analysis software ImageJ (http://rsbweb.nih.gov/ij).

Spectroscopic characterization of c4

CD and fluorescence emission spectra of c4 in its native and urea-denatured state were recorded. Protein samples were incubated in a 50 mM sodium phosphate buffer, containing no denaturant or 1, 2, and 4M urea at 37°C before taking the measurement. The far-ultraviolet CD spectra was recorded in a Jasco J-710 CD Spectropolarimeter (Jasco), averaged over three scans at a spectral bandwidth of 1 nm with 2 s integration time using rectangular fused silica cells with an optical path length of 1 mm. Fluorescence emission spectra was recorded in a PTI Quantamaster 30 Fluorescence Spectrofluorometer (Photon Technology International) with excitation at 280 nm and spectral bandwidths of 2 nm (excitation) and 4 nm (emission) using quartz cuvette (pathlength of 0.1 cm). All spectra were recorded at 37°C and buffer-corrected. The final protein concentration was 5 μM for CD spectra and 0.3 μM for fluorescence emission spectra.

Unfolding and refolding transition

Urea-induced unfolding and refolding transition of the proteins were examined by monitoring the intrinsic tryptophan fluorescence intensity at the emission wavelength of 342 nm using an excitation wavelength of 280 nm. For unfolding transition, proteins, which were previously incubated with no maltose and 5 mM maltose, were denatured at the appropriate urea concentration at 37°C for 1 h in 50 mM phosphate buffer, pH 7.5. For refolding transition, proteins were initially denatured in 7M urea for 30 minutes at 37°C. Renaturation was carried out by incubating the denatured proteins in phosphate buffer containing various concentration of urea for 1 h at 37°C. Fluorescence was measured at the final protein concentration of 50 μM.

Unfolding and refolding kinetics

For unfolding kinetics, protein unfolding was initiated by injecting native proteins into 3 and 5M urea buffer in the absence and presence of maltose respectively, in a thermostated cuvette, to a final protein concentration of 0.3 μM. For unfolding kinetics of proteins with maltose, proteins were initially incubated with 5 mM maltose for 1 h at 37°C before mixing with 5M urea buffer. For refolding kinetics, proteins were denatured in 5M urea buffer for 1 h at 37°C, then refolding was initiated by diluting in refolding buffer, containing 50 mM sodium phosphate and 10% glycerol. For refolding in the presence of maltose, maltose was added to the refolding buffer (5 mM maltose). Tryptophan fluorescence emission spectra were monitored with the emission wavelength of 342 nm and excitation wavelength of 280 nm. All spectra were recorded at 37°C and buffered-corrected.

Acknowledgments

The authors thank Dr. Richard Heins for valuable discussion, and Yang Li and Jesse Placone for assistance with circular dichroism spectrometery.

References

1. Vallee-Belisle A, Plaxco KW (2010) Structure-switching biosensors: inspired by Nature. Curr Opin Struct Biol 20:518–526.
2. Guntas G, Mitchell SF, Ostermeier M (2004) A molecular switch created by in vitro recombination of nonhomologous genes. Chem Biol 11:1483–1487.
3. Guntas G, Mansell TJ, Kim JR, Ostermeier M (2005) Directed evolution of protein switches and their application to the creation of ligand-binding proteins. Proc Natl Acad Sci U S A 102:11224–11229.
4. Wright CM, Majumdar A, Tolman JR, Ostermeier M (2009) NMR characterization of an engineered domain fusion between maltose binding protein and TEM1 beta-lactamase provides insight into its structure and allosteric mechanism. Proteins 78:1423–1430.
5. Sohka T, Heins RA, Phelan RM, Greisler JM, Townsend CA, Ostermeier M (2009) An externally-tunable bacterial band-pass filter. Proc Natl Acad Sci USA 106: 10135–10140.
6. Heins RA, Choi JH, Sohka T, Ostermeier M (2011) In vitro recombination of non-homologous genes can result in gene fusions that confer a switching phenotype to cells. PLoS One 6:e27302.
7. Ramsay D, Bevan N, Rees S, Milligan G (2001) Detection of receptor ligands by monitoring selective stabilization of a Renilla luciferase-tagged, constitutively active mutant, G-protein-coupled receptor. Br J Pharmacol 133:315–323.
8. Muddana SS, Peterson BR (2003) Fluorescent cellular sensors of steroid receptor ligands. Chembiochem 4: 848–855.
9. Moreau MJ, Morin I, Schaeffer PM (2010) Quantitative determination of protein stability and ligand binding using a green fluorescent protein reporter system. Mol Biosyst 6:1285–1292.
10. Wright CM, Wright RC, Eshleman JR, Ostermeier M (2011) A protein therapeutic modality founded on molecular regulation. Proc Natl Acad Sci U S A 108: 16206–16211.
11. Hecht MH, Nelson HC, Sauer RT (1983) Mutations in lambda repressor's amino-terminal domain: implications

for protein stability and DNA binding. Proc Natl Acad Sci U S A 80:2676–2680.
12. Lim WA, Sauer RT (1989) Alternative packing arrangements in the hydrophobic core of lambda repressor. Nature 339:31–36.
13. Lim WA, Sauer RT (1991) The role of internal packing interactions in determining the structure and stability of a protein. J Mol Biol 219:359–376.
14. Kim CS, Pierre B, Ostermeier M, Looger LL, Kim JR (2009) Enzyme stabilization by domain insertion into a thermophilic protein. Protein Eng Des Sel 22:615–623.
15. Watanabe M, Mishima Y, Yamashita I, Park SY, Tame JR, Heddle JG (2008) Intersubunit linker length as a modifier of protein stability: crystal structures and thermostability of mutant TRAP. Protein Sci 17: 518–526.
16. Patel MM, Tzul F, Makhatadze GI (2011) Equilibrium and kinetic studies of protein cooperativity using urea-induced folding/unfolding of a Ubq-UIM fusion protein. Biophys Chem 159:58–65.
17. Schellman JA (1975) Macromolecular binding. Biopolymers 14:999–1018.
18. Pace CN, McGrath T (1980) Substrate stabilization of lysozyme to thermal and guanidine hydrochloride denaturation. J Biol Chem 255:3862–3865.
19. Park C, Marqusee S (2005) Pulse proteolysis: a simple method for quantitative determination of protein stability and ligand binding. Nat Methods 2:207–212.
20. Fukada H, Sturtevant JM, Quiocho FA (1983) Thermodynamics of the binding of L-arabinose and of D-galactose to the L-arabinose-binding protein of Escherichia coli. J Biol Chem 258:13193–13198.
21. Brandts JF, Lin LN (1990) Study of strong to ultratight protein interactions using differential scanning calorimetry. Biochemistry 29:6927–6940.
22. Shrake A, Ross PD (1990) Ligand-induced biphasic protein denaturation. J Biol Chem 265:5055–5059.
23. Celej MS, Dassie SA, Freire E, Bianconi ML, Fidelio GD (2005) Ligand-induced thermostability in proteins: thermodynamic analysis of ANS-albumin interaction. Biochim Biophys Acta 1750:122–133.
24. Cimmperman P, Baranauskiene L, Jachimoviciute S, Jachno J, Torresan J, Michailoviene V, Matuliene J, Sereikaite J, Bumelis V, Matulis D (2008) A quantitative model of thermal stabilization and destabilization of proteins by ligands. Biophys J 95:3222–3231.
25. Kuwajima K, Mitani M, Sugai S (1989) Characterization of the critical state in protein folding. Effects of guanidine hydrochloride and specific Ca2+ binding on the folding kinetics of alpha-lactalbumin. J Mol Biol 206:547–561.
26. Sancho J, Meiering EM, Fersht AR (1991) Mapping transition states of protein unfolding by protein engineering of ligand-binding sites. J Mol Biol 221: 1007–1014.
27. Sugawara T, Kuwajima K, Sugai S (1991) Folding of staphylococcal nuclease A studied by equilibrium and kinetic circular dichroism spectra. Biochemistry 30: 2698–2706.
28. Chiti F, Taddei N, van Nuland NA, Magherini F, Stefani M, Ramponi G, Dobson CM (1998) Structural characterization of the transition state for folding of muscle acylphosphatase. J Mol Biol 283:893–903.
29. Na YR, Park C (2009) Investigating protein unfolding kinetics by pulse proteolysis. Protein Sci 18:268–276.
30. Millet O, Hudson RP, Kay LE (2003) The energetic cost of domain reorientation in maltose-binding protein as studied by NMR and fluorescence spectroscopy. Proc Natl Acad Sci U S A 100:12700–12705.
31. Foit L, Morgan GJ, Kern MJ, Steimer LR, von Hacht AA, Titchmarsh J, Warriner SL, Radford SE, Bardwell JC (2009) Optimizing protein stability in vivo. Mol Cell 36:861–871.
32. Ausubel FM (1987) Current protocols in molecular biology. New York: Wiley.
33. Park C, Marqusee S (2006) Quantitative determination of protein stability and ligand binding by pulse proteolysis. Curr Protoc Protein Sci Chapter 20:Unit 20.11.
34. Kim MS, Song J, Park C (2009) Determining protein stability in cell lysates by pulse proteolysis and Western blotting. Protein Sci 18:1051–1059.